Genetic dissection of the phophoinositide cycle in *Drosophila* photoreceptors

Che-Hsiung Liu[1], Murali K. Bollepalli[1] , Samuel V. Long[1], Sabrina Asteriti[1]., Julie Tan[2,3], Julie A. Brill[2,3], Roger C. Hardie[1].

[1]Cambridge University Department of Physiology Development and Neuroscience

Downing St, Cambridge, CB2 3EG, United Kingdom

[2] Program in Cell Biology, The Hospital for Sick Children, Peter Gilgan Centre for Research and Learning, 686 Bay Street, Room 15.9716, Toronto, ON M5G 0A4, Canada

[3]Department of Molecular Genetics, University of Toronto, Room 4396, Medical Sciences Building, 1 King's College Circle, Toronto, ON M5S 1A8, Canada

Running title *Drosophila* Phosphoinositide cycle

Key words PIP_2, PI4 kinase, PIP5 kinase, phototransduction, TTC7

Address for correspondence

Roger C Hardie Cambridge University Department of Physiology Development and Neuroscience, Downing St Cambridge CB23EG U.K. rch14@cam.ac.uk

Acknowledgements. We are grateful to Drs Armin Huber, Padinjat Raghu and the Vienna Drosophila Resource Center (VDRC) for providing flies. This project received funding from the Biotechnology and Biological Sciences Research Council (RCH, MKB, C-HL, BBSRC Grants BB/G0092531/1 and BB/M007006/1), European Union's Horizon 2020 research and innovation programme (RCH, SA Grant No. 658818-FLYghtCaRe, Canadian Institutes of Health Research (JAB, Grant No. MOP#81187), The Cancer Research Society, Inc. (JAB).) and a SickKids Restracomp scholarship (JT).

Competing interests:The authors declare no competing or financial interests.

Summary statement

Using genetically encoded probes to quantify PIP_2 and PI4P turnover *in vivo*, novel components of the phosphoinositide cycle in *Drosophila* photoreceptors were identified including PI4KIIIα and associated scaffolding proteins.

Abstract

Phototransduction in *Drosophila* is mediated by phospholipase C dependent hydrolysis of PIP_2, and is an important model for phosphoinositide signalling. Although generally assumed to operate by generic machinery conserved from yeast to mammals, some key elements of the phosphoinositide cycle have yet to be identified in *Drosophila* photoreceptors. Here we used transgenic flies expressing fluorescently tagged probes (P4M and Tb^{R332H}), which allow *in vivo* quantitative measurements of PI4P and PIP_2 dynamics in photoreceptors of intact living flies. Using mutants and RNA interference for candidate genes potentially involved in phosphoinositide turnover, we identified *Drosophila* PI4KIIIα (CG10260) as the PI4-kinase responsible for PI4P synthesis in the photoreceptor membrane. Our results also indicate that PI4KIIIα's function requires *rbo* (the *Drosophila* orthologue of Efr3) and CG8325 (orthologue of YPP1), both of which are implicated as scaffolding proteins required for PI4KIIIα activity in yeast and mammals. However, our evidence indicates that the recently reported central role of *dPIP5K59B* (CG3682) in PIP_2 synthesis in the rhabdomeres should be re-evaluated; although PIP_2 resynthesis was suppressed by RNAi directed against *dPIP5K59B*, little or no defect was detected in a reportedly null mutant (*dPIP5K*^{18}).

Introduction

Phosphoinositides such as PtdIns(4,5)P_2 (PIP_2) are ubiquitous and vital regulators of numerous cellular functions (Balla, 2013; Di Paolo and De Camilli, 2006; Hilgemann et al., 2001; Payrastre et al., 2001; Rohacs, 2009; Yin and Janmey, 2003), and their metabolism plays vital roles in most cells. In *Drosophila* photoreceptors, the light response is mediated by a G-protein coupled phospholipase C (PLC) cascade (Hardie, 2012; Hardie and Juusola, 2015; Katz and Minke, 2009; Montell, 2012; Yau and Hardie, 2009). Here, hydrolysis of PIP_2 by PLC results in activation of two Ca^{2+} permeable cation channels: "transient receptor potential" (TRP) - and TRP-like (TRPL), which mediate the electrical response to light (Hardie and Minke, 1992; Montell and Rubin, 1989; Phillips et al., 1992). Along with other core components of the transduction cascade, rhodopsin, PLC and the channels are localised in a stack of plasma membrane microvilli forming the light guiding rhabdomere. Light-activated PLC activity in the photoreceptors is extremely powerful, capable of depleting the entire PIP_2 pool in the microvillar membrane within ~1s, if not controlled by rapid Ca^{2+} and PKC dependent negative feedback (Gu et al., 2005; Hardie et al., 2004; Hardie et al., 2015; Hardie et al., 2001). Appropriate and timely replenishment of PIP_2 is essential not only for maintained visual signalling but also for cell integrity, and photoreceptors undergo degeneration in mutants where PIP_2 levels cannot be maintained (Sengupta et al., 2013). Although specialised for vision, the phosphoinositide cycle in the *Drosophila* eye appears to operate via canonical machinery conserved from yeast to mammals. Because of their experimental accessibility and decades of intensive study, *Drosophila* photoreceptors have long represented an important genetic model for this ubiquitous pathway (Balakrishnan et al., 2015; Hardie, 2012; Hardie and Juusola, 2015; Katz and Minke, 2009; Montell, 2012; Raghu et al., 2012).

Many of the genes for enzymes and other proteins involved in phosphoinositide turnover in *Drosophila* photoreceptors have been at least putatively identified. However, certain elements, such as the kinases required for PtdIns(4)P (PI4P) and PIP_2 synthesis remain to be identified, whilst for some of the others there has been limited direct evidence demonstrating their involvement in phosphoinositide metabolism *in situ*. The most widely used tools used to monitor phosphoinositide turnover in living cells are fluorescently tagged phosphoinositide binding peptides, which rapidly translocate to and from membranes depending on the concentration of their target lipid (Stauffer et al., 1998; Varnai and Balla, 1998; Varnai et al., 2017). Recently we adapted this methodology to the fly retina (Hardie et al., 2015). After testing several probes, we selected Tb^{R332H}, a mutant variant of the pleckstrin homology (PH) domain from the Tubby protein (Hughes et al., 2007; Quinn et al., 2008) as the most reliable probe for PIP_2 in the photoreceptors, whilst the P4M domain of *Legionella* SidM (Hammond et al., 2014) was chosen for PI4P. Importantly, the probes can be quantitatively imaged in the rhabdomeres of intact living flies allowing completely non-invasive measurements of this sub-cellular compartment to be made *in vivo* over many hours.

In the present study we used these probes, in combination with electrophysiological approaches, to screen candidate genes that might be involved in phosphoinositide turnover in photoreceptors, using a combination of mutants and RNA interference. We identify PI4KIIIα as the kinase isoform responsible for PI4P synthesis in the microvilli. Our results also indicate that PI4KIIIα's function requires the additional involvement of orthologues of two genes (Efr3 and YPP1), that have been implicated in PI4KIIIα function in yeast and mammals (Baird et al., 2008; Chung et al., 2015; Nakatsu et al., 2012). Our results also support the identification of two elements previously implicated by other evidence, namely CDP-diaglycerol synthase and PI-synthase. However, our evidence raises questions about the recently reported central role of *dPIP5K59B* (CG3682) in PIP_2 synthesis in the rhabdomeres (Chakrabarti et al 2015).

Results

Using GFP-tagged lipid probes to monitor phosphoinositide turnover *in vivo*

To monitor PIP_2 and PI4P depletion and resynthesis *in vivo* we used flies expressing specific PIP_2 and PI4P fluorescently tagged probes (Tb^{R323H}-YFP and P4M-GFP) in the major photoreceptor class (R1-6) using the promoter for the opsin (Rh1) expressed in these cells (Hardie et al., 2015). As previously described (Hammond et al., 2014; Hardie et al., 2015; Hughes et al., 2007), these probes appear to be specific for PIP_2 (as opposed to $InsP_3$) and PI4P (as opposed to PIP_2) respectively, unlike other probes sometimes used for monitoring PIP_2 (eg PH domain of PLCδ) or PI4P (e.g. PH-domains from FAPP1, OSH1 and OSH2). In otherwise wild-type flies, these probes indicate that both PIP_2 and PI4P are depleted in the rhabdomeres by the blue excitation light with approximately exponential time courses of ~7 s for PIP_2 (using Tb^{R332H}) and ~12 s for PIP (using P4M). Such stimulation also results in saturating, persistent activation of the transduction cascade causing a prolonged depolarizing afterpotential (PDA) due to conversion of the majority (70%) of rhodopsin (R) to the active metarhodopsin (M) state (review Hardie, 1985) and PIP_2 remains depleted until M is photoreisomerised to R by long wavelength light (Hardie et al. 2015). Following rapid (~2 s) photoreisomerisation of M to R, recovery of the respective probes to the microvillar membrane (reflecting resynthesis of PI4P and PIP_2) can be monitored *in vivo* from the recovery of fluorescence of the deep pseudopupil (DPP) in completely intact animals as a function of time in the dark (Fig. 1). Such recordings yield half times (*t½)* of recovery of ~10 s for PI4P and ~40 s for PIP_2 in otherwise wild-type flies.

Because mutations in many of the genes we investigated are organismal or cell-lethal, in many cases we resorted to RNAi knockdown using fly stocks from the Vienna Drosophila Resource Center (VDRC). The UAS-RNAi constructs in these flies must be driven by the Gal4-UAS system (Brand and Perrimon, 1993). In order to achieve strong and selective RNAi knockdown in the eye we

crossed the UAS-RNAi lines to *GMRGal4* flies in which Gal4 expression is driven by the GMR (glass multiple repeats) promoter, which is strongly expressed in all cells of the developing eye (Hay et al., 1997). These flies also expressed a UAS-RNAi construct for the *white* (*w*) gene (*GMRGal4, w-UAS-RNAi*, referred to as *GMRw*), which results in virtually white-eyed flies (Kalidas and Smith, 2002), hence maximizing reporter fluorescence. Recently we reported that expression of one copy of GMRGal4 already induces a number of subtle phenotypes by itself, including a ~ 2-3 fold reduction in sensitivity, shorter ommatidia and a ~ 30% reduction in area of microvillar membrane (Bollepalli et al., 2017). Since PIP_2 turnover had not been investigated in GMRGal4 flies, we first characterised PI4P and PIP_2 turnover in control *GMRw/+* flies using P4M and Tb^{R332H} probes. Although behaviour was broadly similar, the rate of resynthesis of both PI4P (t ½ ~25s cf ~10 s) and PIP_2 (t ½ ~60 s cf ~40 s) were slightly, but significantly ($p < 0.0001$) slower than in wild-type backgrounds (Fig. 1). The kinetics of PI4P depletion in particular was also noticeably faster (Fig. 1D).

As additional controls, we also separately tested all RNAi lines with apparent phenotypes in PIP_2 and/or PI4P resynthesis by crossing them into otherwise wild-type Tb^{R332H} and P4M backgrounds (without *GMRGal4*), but in this case none showed any significant differences to the wild-type controls (Fig. S1). The effectiveness of UAS-RNAi knockdown driven by *GMRGal4* was validated by qRT-PCR on retinal tissue dissected from freeze-dried heads in critical lines showing significant phenotypes (Fig. S2 and see methods).

Genetic dissection of PI turnover

Drosophila contains identified and candidate genes for all of the respective elements of the canonical PI cycle (Fig. 1I). Of these we recently showed that both PI4P and PIP_2 synthesis were severely compromised in mutants of PITP (*rdgB*) and DAG kinase (*rdgA*), providing *in vivo* evidence for their essential role in the cycle, whilst as expected PIP_2 hydrolysis (depletion) is prevented in *norpA* mutants lacking PLC (Hardie et al., 2015). The primary aim of this study was to test the involvement of remaining candidate genes using specific PI4P and PIP_2 probes and thereby provide a more comprehensive overview of the phosphoinositide cycle machinery in the photoreceptors.

PI4 kinase

The *Drosophila* genome contains three putative PI4-kinase genes: *PI4KIIα* (CG2929), *PI4KIIIβ* (*fwd* = CG7004) and *PI4KIIIα* (CG10260), and limited evidence has implicated all three in development and/or degeneration in *Drosophila* retina (Forrest et al., 2013; Raghu et al., 2009). Which isoform is responsible for maintaining the PI4P pool required for phototransduction in the microvillar (plasma membrane) rhabdomeres is not known; however, we suspected PI4KIIIα, because in other organisms and tissues it has been implicated in synthesis of PI4P at the plasma membrane whilst PI4KIIα and IIIβ have been implicated on endomembranes (Balla et al., 2008; Burgess et al., 2012; Polevoy et al.,

2009; Tan et al., 2014). Of the three kinases, PI4KIIIα is also the most strongly eye enriched isoform (7-fold enriched – www.Flyatlas.org).

Because a null mutation (*PI4KIIIα*$^{\Delta 123}$) is lethal, we first tried to generate *PI4KIIIα* null whole-eye mosaics using the FLP-FRT method (Stowers and Schwarz, 1999); however, this resulted in failure of eyes to develop indicating the mutation was also cell-lethal in the developing eye. We also investigated PI4P and PIP_2 resynthesis in *PI4KIIIα*$^{\Delta 123}$ heterozygotes generated by crossing *PI4KIIIα*$^{\Delta 123}$/FM7 flies to flies expressing either P4M or Tb^{R332H} probes (Fig. S3). PIP_2 resynthesis time courses measured in *PI4KIIIα*/+ heterozygotes using the Tb^{R332H} probe were indistinguishable from controls (whether the parent Tb^{R332H} line or *FM7*/+ siblings). PI4P resynthesis measured using P4M-GFP in *PI4KIIIα*/+ heterozygotes appeared to be marginally slower than in sibling controls ($t½$ = 11.3 s cf 9.8 s in controls), but, although significant (p = 0.01), because the difference was so small we would not exclude this being due to other differences in genetic background.

We therefore resorted to RNA interference using UAS-RNAi constructs driven by *GMRGal4* (Fig. 2). RNAi knockdown of either *PI4KIIIβ* (*fwd*) or *PI4KIIα* had no detectable influence on the time course of either PI4P or PIP_2 resynthesis, with the respective probes recovering with half times of ~30 s (P4M), and ~50 s (Tb^{R332H}) indistinguishable from *GMRw* controls. However, RNAi knockdown of PI4KIIIα (reducing transcript levels to ~8% , see Fig. S2), profoundly delayed recovery of both PI4P and PIP_2 ($t½$ ~500 s) suggesting that PI4KIIIα is indeed the main isoform responsible for PI4P synthesis in the rhabdomeres. This also appears to be the PI4P pool required for phototransduction because slow recovery of the probes was mirrored by a similarly slow recovery of the electrical response to light (ERG) after PI4P and PIP_2 depletion induced by 30s intense blue illumination. In fully dark-adapted flies, the response to light was relatively normal, with only a minor reduction in ERG amplitude and sensitivity and reduced synaptic "on" and "off" transients compared to controls (Fig. 3).

We were concerned that PI4KIIIα knockdown might have adversely affected development of the eye; however, there were no obvious structural differences to *GMRw*/+ controls, with facet patterns showing only occasional minor irregularities, which can also be seen in *GMRw*/+ eyes. In terms of photoreceptor structure, dissociated ommatidia prepared for whole-cell recordings were of similar appearance to those from *GMRw*/+ controls, and whole-cell capacitances (a sensitive measure of microvillar surface area) were indistinguishable from *GMRw/+* controls (Fig. S4E). Macroscopic light-induced currents had normal kinetics and at most only slightly (but not significantly) reduced amplitudes compared to *GMRw*/+ controls– though both were reduced, and more variable compared to wild-type (Fig. S4A,B) as previously reported for *GMRGal4* flies (Bollepalli et al., 2017). Single photon responses (quantum bumps) also had normal waveforms, albeit slightly reduced in amplitude

(Fig. S4C,D). These results indicate that the photoreceptors and the basic molecular components of the transduction cascade were essentially intact.

Rolling blackout

Membrane localization and function of PI4KIIIα in yeast and mammals is reported to depend upon association with accessory scaffolding proteins including Efr3, YPP1 and Sfk1 (Baird et al., 2008; Chung et al., 2015; Nakatsu et al., 2012). Interestingly, the *Drosophila* orthologue of Efr3 is *rolling black out* (*rbo*), which was originally suggested to be a DAG lipase by sequence homology of a putative lipase domain (Huang et al., 2004). However, RBO protein has recently been reported to co-immunoprecipitate with PI4KIIIα in *Drosophila*, and has been suggested to be important in controlling PI4P levels in neurons (Zhang et al., 2017). Null *rbo* mutations are lethal, but a temperature-sensitive allele (rbo^{ts}) was reported to have use-dependent defects in the ERG – namely a profound loss of sensitivity to light following bright illumination (Huang et al., 2004). In view of the identification of Efr3 as a scaffolding protein for PI4KIIIα , we asked whether this use-dependent loss of sensitivity might reflect loss of PI4KIIIα function and hence failure to resynthesise PI4P and PIP_2.

To address this we expressed Tb^{R332H} and P4M probes in rbo^{ts} mutants and made measurements at permissive (21-23^o C) and restrictive temperatures (~37^o C). We first compared dark-adapted fluorescence intensities of the reporters at 37^o C and 22^o C in wild-type backgrounds and found that fluorescence at 37^o C was slightly decreased (to ~80% of the level at 22^o C) for both probes, consistent with the known temperature dependence of GFP fluorescence (Zhang et al., 2009). For controls we then investigated the temperature dependence of PIP_2 and PI4P turnover in a wild-type background. As might be expected both PIP_2 and PI4P depletion and resynthesis were accelerated at higher temperatures in wild-type flies (Fig. 4). Thus translocation of Tb^{R332H} out of the rhabdomere during blue excitation (reflecting PIP_2 depletion), had a time constant of ~2s at 37^o C, compared to ~7 s at room temperature (Fig. 4A). Resynthesis was also accelerated with a half-time of fluorescence recovery of ~20s at 37^o C *cf* ~40 s at room temperature (Fig. 4D)). Depletion and resynthesis of PI4P as monitored by P4M were similarly accelerated (Fig. 4C,E). Judging from the F_{max}/F_{min} ratios, the absolute dark-adapted level of both PIP_2 and PI4P at 37^{o}C appeared to be little affected (~95% of levels at 22^{o}C).

In rbo^{ts} mutants, depletion and recovery time courses of PI4P and PIP_2 at 22^o C determined using P4M and Tb^{R332H} probes were similar to those measured in a wild-type background, although P4M recovery in particular was slightly but significantly slower (Fig. 4F). However, when raised to restrictive temperatures, behaviour was profoundly altered (Fig. 4). Fluorescence of the P4M probe declined rapidly already in the dark on raising the temperature to 37^o C and within 3 minutes of activating the heating coil was already reduced to less than 10% of control levels. With shorter

heating periods (90 s - 2 min), more residual P4M fluorescence remained, which then decayed to baseline with a similarly accelerated time course to wild-type controls at 37^{o}C , suggesting that PLC activity was normal. However, thereafter no recovery of fluorescence could be detected in the dark (after the usual M>R reconverting red light) and in most cases fluorescence decreased even further (Fig. 4C,E). This indicates that resynthesis of PI4P in the microvilli is blocked at the restrictive temperature in *rbo*^{ts}, consistent with the notion that RBO (Efr3) is an essential co-factor for PI4KIIIα function.

PIP_2 measured using the Tb^{R332H} probe behaved in a broadly similar fashion, but with some interesting differences. Firstly, PIP_2 (Tb^{R332H} fluorescence) remained at >50% of the original room temperature levels in the rhabdomeres of *rbo*^{ts} eyes for at least 5 minutes at the restrictive temperature in the dark. PIP_2 was then depleted by blue excitation as in wild-type controls, with a similar acceleration in time course (Fig. 4B), again confirming that PLC activity was intact in *rbo*^{ts} at the restrictive temperature. After this initial exposure to blue excitation, there was usually a modest (~25%) recovery of fluorescent probe in the dark over ~200 s (Fig. 4B, D). However, in marked contrast to recoveries in control conditions, rather than inducing the usual decay of any recovered fluorescence, blue excitation now resulted in a slight *increase* in fluorescence with each repeated exposure (Fig. 4B), with an exponential time constant similar to but slightly slower than the initial depletion (tau 3.0 ± 0.3 s, n = 11). Whilst the slight recovery of fluorescence might be taken to indicate partial resynthesis of PIP_2, this would presumably have to come from a source other than PI4P (at least distinct from any pool detected by P4M), whilst the paradoxical increase induced by each light exposure seems hard to explain. An alternative interpretation is that PIP_2 in the rhabdomeres - like PI4P - remained unreplenished, but after the initial depletion of PIP_2 in the rhabdomere by the first episode of blue excitation, each subsequent episode now results in depletion of PIP_2 from plasma membrane outside the microvilli. This could then result in redistribution of some of the probe back to the microvilli, because the probe is expected to report the relative difference in PIP_2 levels between competing sinks (i.e. the rhabdomere and the rest of the plasma membrane). On return to room temperature, both PI4P and PIP_2 turnover remained blocked for at least 30 minutes, but when tested, eventually recovered after a couple of hours.

We also investigated both PI4P and PIP_2 resynthesis with P4M and Tb^{R332H} probes at room temperature following *rbo* RNAi knockdown. Here, we found a very pronounced and significant slowing of both PI4P and PIP_2 resynthesis ($t½$ 248 s for P4M and 173 s for Tb^{R332H}; Fig. 2). As with PI4KIIIα knockdown, the slow or absent recovery of the probes in *rbo*^{ts} and *rbo* RNAi backgrounds was mirrored by very slow and limited recovery of sensitivity following bright illumination as measured in the ERG (Fig. 3D). Indeed in *rbo*^{ts} the majority of flies (9/12) showed no detectable recovery to test flashes for at least 10 minutes following PIP_2 depletion at 37^{o}C.

YPP1 (TTC7)

In yeast and mammals, a second protein (YPP1 in yeast, TTC7 in mammals) is also involved in the scaffolding complex required for PI4KIIIα function (Wu et al., 2014). There appears to be just one orthologue of YPP1/TTC7 in *Drosophila*, annotated as CG8325, but with no reported function. According to Flyatlas (Flyatlas.org) CG8325 is relatively enriched (~3-fold) in both eye and brain tissue. Mutants of CG8325 (*l(2)k14710*) are lethal, therefore we sought evidence for its role by RNA interference using GMRGal4 to drive UAS-*YPP1*-RNAi in flies expressing P4M and Tb^{R332H}. As shown in Fig. 2B,D resynthesis of both PI4P and PIP_2 was severely compromised in these flies. Again this slow recovery was mirrored in a prolonged loss and slow recovery of sensitivity of the light response after bright light adaptation, as measured in the ERG (Fig. 3).

Sfk1 (TMEM150A)

Recently a third regulator of the PI4KIIIα complex was reported, namely Sfk1 (yeast) and its homologue TMEM150A in mammals, which was reported to be required for association of YPP1 with the Efr3/PI4KIIIα complex (Chung et al., 2015). The most closely homologous genes in *Drosophila* are CG4025 (~30% amino-acid identity to TMEM150A) and CG7990 (~20% identity), both of which are enriched in eye and brain tissue (Flyatlas.org). However, using two independent RNAi lines for each gene, we found no obvious effect of either on PI4P or PIP_2 resynthesis (Fig. 2B,D).

CDP-diglyceride synthase (*cds*)

Drosophila cdsA was the first eukaryotic CDP-diglyceride synthase to be cloned and the sole representative in the *Drosophila* genome. It is highly enriched in the retina and has been implicated in the photoreceptor phosphoinositide cycle on the basis that sensitivity to light in the hypomorphic $cdsA^1$ mutant cannot be maintained during and following prolonged exposure to light (Wu et al., 1995). In addition more direct evidence for *cdsA* in microvillar PIP_2 resynthesis came from whole-cell recordings from dissociated photoreceptors in $cdsA^1$ mutants using a genetically targeted electrophysiological PIP_2 biosensor, Kir2.1 (Hardie et al., 2002). To test the requirement of *cdsA* for phosphoinositide recycling *in vivo* we used two independent *cdsA* RNAi lines crossed to *GMRw* flies expressing P4M and Tb^{R332H} probes. In one line (cds^{KK}) PI4P recovery was undetectable, whilst recovery of PIP_2 was extremely slow (t ½ ~800s, Fig. 2). Sensitivity to light and recovery from light adaptation were also greatly compromised in ERG recordings (Fig.3). In the second line (cds^{GD}), PIP_2 recovered to ~50% of original levels relatively quickly (within ~2 minutes), but then took a further ~ 10 minutes to recover to pre-depletion levels, but little or no effect was seen on PI4P recovery times. In these flies sensitivity to light and recovery from light adaptation in ERG recordings were at most

only slightly impaired compared to controls, which is to be expected since 50% PIP_2 levels are sufficient to mediate near maximal activation of TRP channels (Hardie et al., 2015) .

PI synthase

dPIS is the only recognisable homologue of mammalian PI-synthase in the *Drosophila* genome, and has been reported to function as a PI-synthase when heterologously expressed in HEK293 cells (Wang and Montell, 2006). It is expressed in photoreceptors, and mutants have visual phenotypes, including slow recovery of the light response following light adaptation, and hence it is a prime candidate for the PI-synthase in the photoreceptor PI cycle (Wang and Montell, 2006). Because null *dpis* mutants are cell lethal, in order to test the requirement of dPIS for PI synthesis *in vivo*, we again used RNA interference. Resynthesis of both PI4P and PIP_2 in *dpis*-RNAi flies were very substantially slowed ($t½$ 250-400s; Fig. 2B,D), supporting the essential role for dPIS in the photoreceptor phosphoinositide cycle as previously proposed (Wang and Montell, 2006).

PIP5-kinase

In the canonical phosphoinositide cycle (Fig. 1I), the final step in the resynthesis of PIP_2 is conversion of PI4P to PIP_2 *via* PIP5-kinase. The *Drosophila* genome contains genes for two putative PIP5K isoforms: *skittles* (*sktl*) and *dPIP5K59B* (CG3682, shortened hereafter to *dPIP5K*). Both are expressed in the eye, and dPIP5K at least has been reported to immunolocalise to the rhabdomere (Chakrabarti et al. 2015). Severe or null mutations of both genes are organismal lethal or semi-lethal. Null *sktl* mutations are also cell lethal, but it is possible to generate viable whole eye mosaics of a reportedly null *dPIP5K* mutant ($dPIP5K^{18}$) using the FLP-FRT method (Chakrabarti et al., 2015). Using such mosaics, Chakrabarti et al. (2015) recently reported defects in the electrical light response as well as PIP_2 resynthesis and concluded that dPIP5K is the main kinase responsible for the synthesis of PIP_2 required for phototransduction in the rhabdomeres. However, technical issues (Hardie et al., 2015 and see discussion) led us to question some of their findings. We therefore re-examined PIP_2 resynthesis in $dPIP5K^{18}$ eye mosaics using flies provided by the authors of the Chakrabarti et al. (2015) study, confirming their genotype by the effective absence (< 1%) of *dPIP5K* mRNA in dissected retinae using qRT-PCR (Fig. S2C).

In marked contrast to Chakrabarti et al. (2015), when we monitored PIP_2 in $dPIP5K^{18}$ mosaic eyes using Tb^{R332H}, we found robust PIP_2 resynthesis with at most only a slight slowing of the time course of recovery, which was significant with respect to wild-type ($t½$ ~49 s cf 38 s, $p = 0.0002$), but not with respect to sibling heterozygote controls ($t½$ 44 s $p = 0.06$; Fig. 5). Chakrabarti et al. (2015) also reported that over-expression of *dPIP5K* driven by Rh1Gal4 resulted in a marked acceleration of PIP_2 resynthesis; however, when we measured PIP_2 resynthesis using Tb^{R332H} in the same over-expressing

flies we found the time course if anything slower, though statistically indistinguishable from controls (p = 0.14, Fig. 5B,C).

Chakrabarti et al. (2015) also reported a "profound" (*sic*) impairment of the photoreceptor response as inferred from ERG recordings in *dPIP5K*^{18} eye mosaic mutants. We confirmed a similar reduction in ERG amplitudes (Fig. 6); however, the most conspicuous aspect of the *dPIP5K*^{18} phenotype (also noted by Chakrabarti et al. 2015) was the complete lack of the synaptic "on" and "off" transients, which derive from postsynaptic interneurons (LMC's). Recently, another mutant defective in synaptic transmission (*hdc*, which lacks the photoreceptor neurotransmitter histamine) was found to have similarly reduced ERG amplitudes (Fig. 6), suggesting that synaptic feedback from interneurons to photoreceptors normally contributes to the photoreceptor component of the ERG (Dau et al., 2016). Therefore from these results it is not clear whether there is in fact any defect at the level of phototransduction. To investigate this directly, we examined *dPIP5K*^{18} mutant photoreceptors using whole-cell recordings of light-induced currents from dissociated ommatidia (Fig. 7). Morphologically, the mutant ommatidia appeared normal in appearance, and their capacitances (a sensitive measure of microvillar membrane area) were indistinguishable from wild-type (64 ± 8 pF cf 63 ± 5pF, n = 10-13 cells). Importantly, we failed to detect any phenotype at all in the responses to light: absolute sensitivity, responses to single photons, brief flashes and 1 s steps of increasing intensity were all indistinguishable from wild-type, or *dPIP5K*^{18}/+ sibling heterozygote controls (Fig. 7). These results indicate that *dPIP5K*^{18} mutants have no detectable defects in phototransduction and at most marginal defects in PIP_2 synthesis in the rhabdomere. By contrast, the complete lack of synaptic transients in the ERG suggests that *dPIP5K*^{18} mutants may be defective in PIP_2 synthesis at synaptic terminals where PIP_2 is believed to be critical for normal vesicular exo- and endocytosis, and interacts with key synaptic proteins such as synaptotagmin (Di Paolo et al., 2004; Lauwers et al., 2016; Park et al., 2015).

The *dPIP5K*^{18} mutant was generated by a targeted "insertion of a selection marker (*Pw*$^{+}$) flanked by multiple stop codons within the gene such that the kinase domain of *dPIP5K* was disrupted" (*sic*) and lack of protein was confirmed by Western blot (Chakrabarti et al., 2015). Nevertheless, we also proceeded to measure PIP_2 resynthesis using UAS-*dPIP5K*-RNAi (VDRC line 108104KK). Surprisingly, despite the virtual lack of effect of the *dPIP5K*^{18} mutation, PIP_2 resynthesis measured using Tb^{R332H} was in fact markedly slower in UAS-*dPIP5K*-RNAi flies crossed to *GMRw* ($t½$ 430 s, Fig. 2A,B). This effect seemed to be specific for PIP_2 as PI4P resynthesis measured using P4M was relatively little affected (Fig. 2C,D). This suggests either that the *dPIP5K*^{18} mutant was not null as reported (Chakrabarti et al. 2015) or that UAS-*dPIP5K*-RNAi had influenced PIP_2 resynthesis by off-target effects.

The second *PIP5K* gene in *Drosophila* is *sktl* (*skittles*). Severe alleles, such as $sktl^{\Delta 1-1}$ or $sktl^{\Delta 20}$ are lethal (Hassan et al., 1998), and attempts to generate whole-eye mosaics with $sktl^{\Delta 1-1}$ resulted in failure of eyes to develop, indicating it is cell lethal in the developing eye (see also Chakrabarti et al., 2015). Trans-heterozygotes ($sktl^{\Delta 1-1}/sktl^{\Delta 20}$) are viable with eyes of normal appearance, but when we expressed Tb^{R332H} in $sktl^{\Delta 1-1}/sktl^{\Delta 20}$ trans-heterozygotes, PIP_2 resynthesis time course was not obviously affected (Fig. S3E). Neither did we find any obvious slowing of resynthesis in single or double heterozygotes of *dPIP5K* and $sktl^{\Delta 1-1}$ (Fig. S3). Finally, we measured PIP_2 resynthesis time courses in UAS-*sktl* RNAi flies (crossed to *GMRw*) and found a slight slowing with respect to *GMRw* controls ($t½$ 88 s cf 67 s), which was significant on a direct *t*-test , but not on a 1 way-Anova comparing all the RNAi lines (Fig. S3F). However, uniquely amongst the RNAi lines we tested, qRT-PCR of dissected retina revealed no significant knockdown of *sktl* mRNA in these flies (Fig. S2). In the absence of data from true null alleles or a validated RNAi line, we are reluctant to draw any conclusions from these results, leaving open the possibility that *sktl* may contribute to PIP_2 synthesis in the rhabdomeres.

Discussion

We have developed transgenic flies and methodology that allow quantitative measurements of phosphoinositide turnover in the microvillar rhabdomeres of completely intact living flies (Hardie et al., 2015). In the present study we used this approach to screen for candidate genes that might be involved in maintaining phosphoinositide levels in the rhabdomeres. Because least is known about them in the *Drosophila* eye, much of our study concentrated upon the kinases presumed to be responsible for synthesis of PI4P and PIP_2 (PI4-kinase and PIP5-kinase).

The PI4-kinase required for phototransduction had not previously been identified in *Drosophila* photoreceptors, although PI4KIIα has been implicated in rhabdomere biogenesis (Raghu et al., 2009), whilst downregulation of either PI4KIIIβ (*fwd*) or PI4KIIIα by RNAi partially rescued retinal degeneration caused by upregulation of PI4P (Forrest et al., 2013). However, PI4KIIIα has consistently been identified as the isoform associated with plasma membrane PI4P pools (Balla et al., 2008; Balla, 2013; Tan and Brill, 2014) and our evidence now strongly supports the identification of PI4KIIIα as the isoform responsible for maintaining the "phototransduction pool" of PI4P in the rhabdomeres. Firstly, using RNAi, we found profound slowing of both PI4P and PIP_2 resynthesis following PI4KIIIα knockdown, whilst RNAi directed against the other two candidates had no effect. This slowing down of PI4P and PIP_2 resynthesis was mirrored in a similarly slow recovery of the light response following bright illumination. Secondly, PI4KIIIα activity in both yeast and mammals has recently been found to be critically dependent upon a scaffolding complex including Efr3 and YPP1 (= TTC7 in mammals), and mutant and/or RNAi knockdown of the respective *Drosophila* orthologues

421 of both these genes was found to have very similar effects in blocking or profoundly slowing PI4P
422 and PIP_2 resynthesis and recovery of light sensitivity.
423
424 The *Drosophila* orthologue of Efr3 is *rolling black out* (*rbo*, also referred to as *stmA*). Previously it
425 was found that the temperature-sensitive rbo^{ts} mutant showed a complete loss of light response
426 following bright illumination (Huang et al., 2004) and an acute blockade of synaptic transmission
427 (Huang et al., 2006), but at that time the only homology noted was to DAG lipase, whilst *in vitro*
428 biochemistry on whole heads appeared to show an accumulation of PIP_2 leading the authors to suggest
429 that RBO lipase activity was somehow required for PLC function. By contrast, our results using both
430 rbo^{ts} mutants and *rbo* RNAi indicated that PLC activity (as witnessed by the initial rapid translocation
431 of both Tb^{R332H} and P4M probes) was normal at the restrictive temperature, but PI4P (and
432 consequently PIP_2) failed to be resynthesised, strongly supporting a role in PI4KIIIα function. A
433 similar block of both PI4P and PIP_2 resynthesis was obtained following RNAi knockdown of the
434 *Drosophila* YPP1 orthologue (CG8325). In yeast and mammals yet another regulator of the PI4KIIIα
435 complex has been reported (Sfk1, or TMEM150A in mammals). In contrast to *rbo* and YPP1 the
436 *Drosophila* genome does not contain an obvious orthologue of this protein, and RNAi knockdown of
437 the two most closely related genes, with 20% (CG7790) or 30% (CG4025) amino-acid identity
438 respectively, had no obvious effect. However, little can be concluded from this negative result and we
439 do not, for example, exclude the possibility that both can contribute in a redundant manner. Overall
440 though, our evidence supports the existence of a PI4KIIIα/Efr3/YPP1 complex in flies and indicates
441 that it is essential for both PI4P and downstream PIP_2 synthesis in the microvillar membrane.
442 Because null mutations of all three genes are lethal in the fly, this complex can also be expected to be
443 of more widespread function.
444
445 The situation with PIP5-kinase is less clear. Recently Chakrabarti et al. (2015) concluded that dPIP5K
446 was the key kinase required for synthesis of PIP_2 required for phototransduction. They showed that
447 dPIP5K immunolocalised to the rhabdomeres, and reported a severe defect in PIP_2 resynthesis
448 measured with a fluorescent probe (PLCδ-PH-GFP) in $dPIP5K^{18}$ mutants. However, even their wild-
449 type recovery times (~3-4 minutes) were much slower than should be the case with this probe (~ 20
450 sec, see Hardie et al 2015). This suggests that their measurements were compromised, most likely by
451 failure to rapidly reconvert M to R after blue excitation, so that in effect they may have been
452 measuring the rate of M to R photoreisomerisation by continuous red light rather than PIP_2 synthesis
453 (see Hardie et al., 2015 for further discussion). Using the Tb^{R332H} probe, and ensuring rapid M to R
454 photoreisomerisation, our results reveal at most only a very minor slowing of PIP_2 resynthesis in the
455 same $dPIP5K^{18}$ mutants. Chakrabarti et al. (2015) also reported "profound defects" in ERG recordings
456 from $dPIP5K^{18}$ mutants. However, although we confirmed the same ERG phenotype, we attribute this

to a defect in synaptic transmission, whilst photoreceptor light responses were quantitatively indistinguishable from controls when studied using more direct whole-cell recording techniques.

Surprisingly, despite the virtual lack of effect of the *dPIP5K*^{18} mutation, *dPIP5K*-RNAi *did* result in a very pronounced slowing of PIP_2 resynthesis. This discrepancy is perplexing and would seem to imply either that *dPIP5K*-RNAi had unanticipated off-target effects (although this did not appear to include *sktl* mRNA; Fig. S2B), or that the *dPIP5K*^{18} mutation was not null. *dPIP5K* has multiple transcripts, and, although our qRT-PCR primers should have detected all the transcripts reported in the databases (Flybase.org), the existence of an unrecognised transcript that was not eliminated by the mutation cannot be excluded. Another possibility would be compensatory up-regulation of alternative gene(s) in the *dPIP5K*^{18} mutant, but not in *dPIP5K*-RNAi flies, although again, this did not appear to include *sktl* (Fig S2C) .

In conclusion, identification of the PIP-kinase responsible for the synthesis of PIP_2 required for phototransduction still requires further investigation. Because of the RNAi effects reported here, *dPIP5K* (CG3682) still remains a viable candidate; but only, it would seem, on the assumption that *dPIP5K*^{18} is not a null mutant. Because we were unable to generate viable *sktl* null mutants, and because *sktl* RNAi failed to suppress mRNA (Fig. S2), we cannot exclude a role for *sktl*, and one possibility is that PIP_2 synthesis may be mediated by both *dPIP5K* and *sktl* in a redundant manner. In principle PIP_2 could also be synthesised from PI5P via PI5P 4-kinase (*dPIP4K*). However, synthesis via this route would be difficult to reconcile with the requirement for PI4-kinase (and hence PI4P) for PIP_2 synthesis indicated in the present study. Furthermore, null mutants of *dPIP4K* have essentially normal light responses (Chakrabarti et al., 2015).

We also tested two further genes previously strongly implicated in the PI cycle, namely *cdsA* and *dPIS*: in both cases we confirmed a profound slowing of PI4P and PIP_2 resynthesis following RNAi knockdown. Together with previous results (e.g. Hardie et al., 2015) , and with the exception of the uncertainty over PIP5 kinase, the forward PI cycle in fly photoreceptors (Fig. 1I) can now be confidently populated with specific genes. However, some reverse steps, in particular PIP_2 and PIP phosphatases, which are likely to be important in determining absolute PI4P and PIP_2 levels, remain to be identified. Finally, we emphasise that *in vivo* measurements using Tb^{R332H} and P4M are, in principle, simple and routine to perform and should lend themselves to further investigations aimed at identifying and characterising the molecular and cellular machinery underlying this important and ubiquitous pathway.

Material and methods

Flies *Drosophila melanogaster* were reared in the dark at 25°C on standard (cornmeal/ agar/ yeast/ glucose) diet. All flies were on white-eyed (w^{1118}) background, but in most cases with one or more Pw^+ transfection marker transgenes, resulting in eyes with an orange colour that varied slightly according to the line in question. Stocks used are listed in Table 1. To monitor phosphoinositide levels in the rhabdomeres, we used flies expressing the PIP_2 specific probe Tb^{R332H} (eYFP-tagged), and the PI4P specific probe P4M (eGFP tagged) in their photoreceptors under control of the rhodopsin (*ninaE*) promoter (Hardie et al., 2015). For RNA interference, UAS-RNAi constructs in VDRC lines (Table 1) were driven by crossing to flies expressing Tb^{R332H} or P4M (on the second chromosome) and *GMRGal4* on the third chromosome, together with *w*-UAS-RNAi to suppress expression of the *w* gene (combination referred to as *GMRw*), thus generating flies with very pale orange eye colour. The resulting F1 progeny used for experiments therefore had one copy of *GMRw*, one copy of the respective UAS-RNAi construct and one copy of Tb^{R332H} or P4M. Controls included flies expressing reporters with just one copy of *GMRw* but no other RNAi construct and also flies expressing one copy of the UAS-RNAi construct, (but not *GMRw*).

The $dPIP5K^{18}$ mutant and *dPIP5K* overexpressing line were kindly provided by the authors of the Chakrabarti et al. (2015) study. In the absence of information on the precise location of the disrupting insert, we checked the genotype of $dPIP5K^{18}$ by qRT-PCR of mosaic retinae, and found that they contained only trace (0.8%) levels of *dPIP5K* mRNA attributable to contaminating tissue in the dissected retinae (Fig. S2C). In addition, as reported, $dPIP5K^{18}$ mutants were homozygous lethal/semi-lethal and retained the Pw^+ selection marker, whilst mosaic retinae reproduced the ERG phenotype reported by Chakrabarti et al.(2015).

Live imaging of the deep pseudopupil and calibration Fluorescence from the deep pseudopupil (DPP) of intact flies was measured as previously described (Hardie et al., 2015). Briefly, flies were fixed with low melting point wax in truncated pipette tips, mounted on a micromanipulator and observed with a 20x/0.35 NA Fluor objective on a Nikon inverted microscope (Nikon Kingston-Upon-Thames UK). The DPP was cropped via a rectangular diaphragm and fluorescence intensity measured using a photomultiplier tube (Cairn Research Ltd, Faversham UK) collecting fluorescence excited by a blue (470 nm peak) ultrabright LED (Cairn Research) and imaged via 515 nm dichroic and OG515 long pass filters. Fluorescence signals were sampled at $\geq$100 Hz and analysed using pClamp10 software (Molecular Devices, CA USA). Unless otherwise stated, data were normalised between F_{max} (from "naïve" dark-adapted flies or maximum fluorescence after recovery, whichever was greatest) and F_{min} (minimum fluorescence after depletion by blue excitation). Photo-reisomerisation of M to R was achieved by long wavelength light delivered by an ultrabright orange/red LED (640 nm Thorlabs Ely, UK) via the microscope eyepiece for 2-4 sec. In some

genotypes, there was sufficient expression of the *w* gene for there to be significant contribution of the intracellular pupil pigment to the recorded signals. When activated, this rapidly migrates towards the rhabdomeres, causing a rapid (tau *ca*. 1-2 s) decrease in fluorescence. Where this was a potential problem, immediately before each episode of blue excitation, the eye was stimulated for 5-7 s with green (540 nm) light of just sufficient intensity to fully activate the pupil (and hence nullify any differential effect on the fluorescence), but insufficient to cause any significant PIP_2 or PI4P depletion. Surprisingly, flies showing a significant pupil effect included those on a *GMRw* background, despite having only a very pale orange eye colour.

Fly rhodopsin (R) absorbs maximally at 480 nm, and the metarhodopsin state (M) at ~570 nm. The two states are thermostable, photo-interconvertible and exist in a photoequilibrium determined by their photosensitivity spectra and the spectral content of illumination (Minke and Kirschfeld, 1979). Photoequilibration was achieved within <100 ms for the blue excitation LED (generating ~70% M, 30% R) and ~2 s for the orange/red LED (generating ~1-2%M, 98-99% R).

Electrophysiology Electroretinograms (ERGs) were recorded as described previously (e.g. Satoh et al., 2010) from flies immobilised as for optical recordings with low melting point wax in truncated pipette tips. Recordings were made using a DAM60 amplifier (World Precision Instruments Hitchin UK) with low resistance (~10 MΩ) glass microelectrodes filled with fly Ringer (140 mM NaCl, 5 mM KCl, 1.5 mM $CaCl_2$, 4 mM $MgCl_2$, 25 mM proline, 5 mM alanine) inserted into the eye, with a similar electrode inserted into the head capsule near the ocelli as reference. Stimulation was via an ultrabright red LED (640nm) or white power LED filtered with broadband Schott filters presented at a distance of ~ 5 mm from the eye via a liquid-filled light guide. Whole-cell patch clamp recordings from photoreceptors in dissociated ommatidia were made as previously described (Hardie et al., 2001; Katz et al., 2017) using 10-15MΩ patch pipettes containing (in mM) 140 K gluconate, 4 MgATP, 1 NAD, 0.4 NaGTP and 10TES with the bath solution described above (chemicals from Sigma Aldrich Gillingham, UK). Illumination, via a green (520 nm) LED was calibrated in effectively absorbed photons by counting quantum bumps (Henderson et al., 2000).

Heating coil For ERG and *in vivo* fluorescence measurements at 37^{o} C , the tip of the plastic pipette containing the mounted fly was inserted into a coil of nichrome resistance wire connected to an Iso-Tech 303DD DC power supply (RS Components Corby, UK), and constant current applied until the desired temperature was reached. Temperature calibration was performed using a thermistor probe of similar size (1 mm diam) to a fly, inserted into the same truncated plastic pipette tip used for ERG or DPP imaging. After activating the heating coil with the appropriate current, the desired temperature of 37^{o}C was reached within ~90-120 s. Unless otherwise stated, fluorescent measurements were started 3 minutes after activating the coil.

qRT-PCR validation

Preparations of nearly pure *Drosophila* retinal tissue were collected as previously described (Matsumoto et al., 1982; Raghu et al., 2000). Briefly, whole flies were snap frozen in liquid nitrogen and dehydrated in pre-chilled acetone at -20^{0}C for 4 days. The acetone was then drained off and retinae were cleanly separated at the level of the basement membrane using forceps and a flattened insect pin. Total RNA was extracted by RNeasy Plus Micro kit (Qiagen Manchester UK) from 20-30 retinae per sample, collected as described above and homogenized by a tissueLyser (Qiagen Manchester UK) with the buffer provided from RNeasy kit and 8 1mm ZIRCONIA beads (Thistle) three times for 50s. Samples were then transferred to a Qiashredder (Qiagen Manchester UK) to remove the debris, and total RNA extracted according to the manufacturer's kit instructions. The nucleic acid preparations were quantitated by absorbance measurements at 260 nm using a nano Drop instrument. Quantitative real time qRT-PCR was performed by One-Step SYBR PrimeScript RT-PCR Kit II (Perfect Real Time) (Takara, Cat No: RR086A) and ABI 7500 fast instrument (Applied Biosystems Warrington UK) using primers listed below.

Ef1a48D forward: 5'-TCCTCCGAGCCACCATACAG-3'
Ef1a48D reverse: 5'- GTCTTGCCGTCAGCGTTACC-3' (used for internal control).

For each respective RNAi line, the primers used were as follows,
rbo forward: 5'- ATAGATAAGTTGGCGCTGGG-3'
rbo reverse: 5'- GGGTGATCGGTCTGGTTAAG-3',
YPP1 forward:5'- AGGAAAAGCACTCAGACACC-3'
YPP1 reverse :5'- TTCACTCAGAGCCTGTTCAAC-3',
dPIP5K forward:5'- AGATACCCTCCCCGCTTAA-3'
dPIP5K reverse:5'- TGGTGAATCTTGCCACTGC-3',
sktl forward:5'- CCTCTAGCAAACTATTCCCTCG-3'
sktl reverse:5'- TCCAGCGGTTCATTCTCATC-3',
PI4KIIIα forward:5'- CAGTATGCCGTAAAGACCCTC-3'
PI4KIIIα reverse:5'- GTGTGCCACTATCTGCGAC-3'.

Statistics Statistical tests (2-tailed unpaired *t*-tests or 1-way ANOVAs with post-tests as specified in text and/or figure legends) were performed in GraphPad Prism5. All errors are expressed as standard errors of the mean (s.e.m.).

602

603

Genotype	***description***	***comment***	***reference***
w^{1118}	white-eyed	"wild-type" stock (Oregon)	
P{w$^+$,ninaE-Tb^{R332H}-YFP}	PIP_2 specific probe under control of Rh1 (*ninaE*) promoter	Referred to as Tb^{R332H}	(Hardie et al., 2015)
P{w$^+$,ninaE-P4M-GFP}	PI4P specific probe under control of Rh1 promoter	Referred to as P4M	(Hardie et al., 2015)
rbo^{ts} (aka *stma^1*)	Temperature sensitive *rbo* mutant (Efr3 orthologue)	Bloomington stock: #34517	(Huang et al., 2004)
FRT42D,dPIP5K^{18}/Cy	Semi-lethal *dPIP5K59B* mutation on FRT42D chromosome	From P Raghu	(Chakrabarti et al., 2015)
FRT42D,GMR-hid,l(2)CL-R/Cy; ey-Gal4,UAS-FLP	Eye lethal flippase line crossed to above to make whole-eye mosaics	Bloomington stock #5251	(Stowers and Schwarz, 1999)
PI4KIIIα$^{\Delta 123}$/FM7	Null mutant (lethal)		(Tan et al., 2014)
P{GSV1}PIP5K59B^{GS2280}/SM1	dPIP5K overexpressing line	Kyoto stock: # 200386	(Chakrabarti et al., 2015)
FRT42D,sktl$^{\Delta 1.1}$/Cy	Lethal *sktl* allele		(Hassan et al 1998)
sktl$^{\Delta 20}$/Cy	Lethal *sktl* allele		(Hassan et al 1998)
Tb^{R332H};GMRGal4,wUAS-RNAi	PIP_2 probe on *GMRw* background	For crossing to UAS RNAi stocks	
P4M; GMRGal4,wUAS-RNAi	PI4P probe on *GMRw* background	For crossing to UAS-RNAi stocks	
VDRC UAS-RNAi stocks	***CG number***	***VDRC ID number***	
KK progenitor	KK progenitor control	10000KK	
PI4KIIIα	CG10260	105614KK	
PI4KIIα	CG2929	110687KK	
fwd (*PI4KIIIβ*)	CG7004	110159KK	
dPIS	CG9245	106842KK	
sktl	CG9985	101642KK	
dPIP5K59B	CG3682	108104KK	
YPP1 orthologue	CG8325	35881GD	
rbo	CG8739	47751GD	
sfk1 homologue	CG4025	100288KK,6924GD	
sfk1 homologue	CG7990	102269KK,46157GD	
cdsA	CG7962	103415KK,5121GD	

Table 1 Fly stocks used in this study (all on *w^{1118}* background).

References

Baird, D., Stefan, C., Audhya, A., Weys, S. and Emr, S. D. (2008). Assembly of the PtdIns 4-kinase Stt4 complex at the plasma membrane requires Ypp1 and Efr3. *J Cell Biol* **183**, 1061-74.

Balakrishnan, S. S., Basu, U. and Raghu, P. (2015). Phosphoinositide signalling in Drosophila. *Biochim Biophys Acta* **1851**, 770-784.

Balla, A., Kim, Y. J., Varnai, P., Szentpetery, Z., Knight, Z., Shokat, K. M. and Balla, T. (2008). Maintenance of hormone-sensitive phosphoinositide pools in the plasma membrane requires phosphatidylinositol 4-kinase IIIalpha. *Mol Biol Cell* **19**, 711-21.

Balla, T. (2013). Phosphoinositides: tiny lipids with giant impact on cell regulation. *Physiol Rev* **93**, 1019-137.

Bollepalli, M. K., Kuipers, M. E., Liu, C. H., Asteriti, S. and Hardie, R. C. (2017). Phototransduction in *Drosophila* is compromised by Gal4 expression but not by $InsP_3$ Receptor knockdown or mutation. *eNeuro* **4**. d.o.i 10.1523/ENEURO.0143-17.2017

Brand, A. H. and Perrimon, N. (1993). Targeted gene expression as a means of altering cell fates and generating dominant phenotypes. *Development* **118**, 401-15.

Burgess, J., Del Bel, L. M., Ma, C. I., Barylko, B., Polevoy, G., Rollins, J., Albanesi, J. P., Kramer, H. and Brill, J. A. (2012). Type II phosphatidylinositol 4-kinase regulates trafficking of secretory granule proteins in Drosophila. *Development* **139**, 3040-50.

Chakrabarti, P., Kolay, S., Yadav, S., Kumari, K., Nair, A., Trivedi, D. and Raghu, P. (2015). A dPIP5K dependent pool of phosphatidylinositol 4,5 bisphosphate (PIP2) is required for G-protein coupled signal transduction in *Drosophila* photoreceptors. *PLoS Genet* **11**, DOI:10.1371/journal.pgen 1004948.

Chung, J., Nakatsu, F., Baskin, J. M. and De Camilli, P. (2015). Plasticity of PI4KIIIalpha interactions at the plasma membrane. *EMBO Rep* **16**, 312-20.

Dau, A., Friederich, U., Dongre, S., Li, X., Bollepalli, M. K., Hardie, R. C. and Juusola, M. (2016). Evidence for Dynamic Network Regulation of Drosophila Photoreceptor Function from Mutants Lacking the Neurotransmitter Histamine. *Front Neural Circuits* **10**, 19. DOI:10.3389/fncir.2016.00019

Di Paolo, G. and De Camilli, P. (2006). Phosphoinositides in cell regulation and membrane dynamics. *Nature* **443**, 651-7.

Di Paolo, G., Moskowitz, H. S., Gipson, K., Wenk, M. R., Voronov, S., Obayashi, M., Flavell, R., Fitzsimonds, R. M., Ryan, T. A. and De Camilli, P. (2004). Impaired PtdIns(4,5)P2 synthesis in nerve terminals produces defects in synaptic vesicle trafficking. *Nature* **431**, 415-22.

Forrest, S., Chai, A., Sanhueza, M., Marescotti, M., Parry, K., Georgiev, A., Sahota, V., Mendez-Castro, R. and Pennetta, G. (2013). Increased levels of phosphoinositides cause neurodegeneration in a *Drosophila* model of amyotrophic lateral sclerosis. *Hum Mol Genet* **22**, 2689-704.

Gu, Y., Oberwinkler, J., Postma, M. and Hardie, R. C. (2005). Mechanisms of light adaptation in *Drosophila* photoreceptors. *Curr Biol* **15**, 1228-34.

Hammond, G. R., Machner, M. P. and Balla, T. (2014). A novel probe for phosphatidylinositol 4-phosphate reveals multiple pools beyond the Golgi. *J Cell Biol* **205**, 113-26.

Hardie, R. C. (1985). Functional organization of the fly retina. *Prog Sens Physiol* **5**, 1-79.

Hardie, R. C. (2012). Phototransduction mechanisms in *Drosophila* microvillar photoreceptors. *WIRES Membr Transp Signal* **1**, WIREs Membr Transp Signal 2012, 1:162–187. doi: 10.1002/wmts.20.

Hardie, R. C., Gu, Y., Martin, F., Sweeney, S. T. and Raghu, P. (2004). In vivo light-induced and basal phospholipase C activity in *Drosophila* photoreceptors measured with genetically targeted phosphatidylinositol 4,5-bisphosphate-sensitive ion channels (Kir2.1). *J Biol Chem* **279**, 47773-82.

Hardie, R. C. and Juusola, M. (2015). Phototransduction in *Drosophila*. *Curr Opin Neurobiol* **34C**, 37-45.

Hardie, R. C., Liu, C. H., Randall, A. S. and Sengupta, S. (2015). In vivo tracking of phosphoinositides in *Drosophila* photoreceptors. *J Cell Sci* **128**, 4328-4340.

Hardie, R. C., Martin, F., Cochrane, G. W., Juusola, M., Georgiev, P. and Raghu, P. (2002). Molecular basis of amplification in *Drosophila* phototransduction. Roles for G protein, phospholipase C, and diacylglycerol kinase. *Neuron* **36**, 689-701.

Hardie, R. C. and Minke, B. (1992). The *trp* gene is essential for a light-activated Ca^{2+} channel in *Drosophila* photoreceptors. *Neuron* **8**, 643-51.

Hardie, R. C., Raghu, P., Moore, S., Juusola, M., Baines, R. A. and Sweeney, S. T. (2001). Calcium influx via TRP channels is required to maintain PIP_2 levels in *Drosophila* photoreceptors. *Neuron* **30**, 149-59.

Hassan, B. A., Prokopenko, S. N., Breuer, S., Zhang, B., Paululat, A. and Bellen, H. J. (1998). skittles, a *Drosophila* phosphatidylinositol 4-phosphate 5-kinase, is required for cell viability, germline development and bristle morphology, but not for neurotransmitter release. *Genetics* **150**, 1527-37.

Hay, B. A., Maile, R. and Rubin, G. M. (1997). P element insertion-dependent gene activation in the *Drosophila* eye. *Proc Natl Acad Sci U S A* **94**, 5195-200.

Henderson, S. R., Reuss, H. and Hardie, R. C. (2000). Single photon responses in *Drosophila* photoreceptors and their regulation by Ca^{2+}. *J Physiol Lond* **524**, 179-194.

Hilgemann, D. W., Feng, S. and Nasuhoglu, C. (2001). The complex and intriguing lives of PIP2 with ion channels and transporters. *Sci STKE* **2001**, RE19.

Huang, F. D., Matthies, H. J., Speese, S. D., Smith, M. A. and Broadie, K. (2004). Rolling blackout, a newly identified PIP_2-DAG pathway lipase required for *Drosophila* phototransduction. *Nat Neurosci* **7**, 1070-8.

Huang, F. D., Woodruff, E., Mohrmann, R. and Broadie, K. (2006). Rolling blackout is required for synaptic vesicle exocytosis. *J Neurosci* **26**, 2369-79.

Hughes, S., Marsh, S. J., Tinker, A. and Brown, D. A. (2007). PIP(2)-dependent inhibition of M-type (Kv7.2/7.3) potassium channels: direct on-line assessment of PIP(2) depletion by Gq-coupled receptors in single living neurons. *Pflugers Arch* **455**, 115-24.

Kalidas, S. and Smith, D. P. (2002). Novel genomic cDNA hybrids produce effective RNA interference in adult *Drosophila*. *Neuron* **33**, 177-84.

Katz, B., Gutorov, R., Rhodes-Mordov, E., Hardie, R. C. and Minke, B. (2017). Electrophysiological Method for Whole-cell Voltage Clamp Recordings from *Drosophila* Photoreceptors. *J Vis Exp*, doi 10.3791/55627.

Katz, B. and Minke, B. (2009). *Drosophila* photoreceptors and signaling mechanisms. *Front Cell Neurosci* **3**, 2. doi 10.3389/neuro.03.002.2009

Lauwers, E., Goodchild, R. and Verstreken, P. (2016). Membrane Lipids in Presynaptic Function and Disease. *Neuron* **90**, 11-25.

Matsumoto, H., Otousa, J. E. and Pak, W. L. (1982). Light-induced modification of *Drosophila* retinal polypeptides in vivo. *Science* **217**, 839-841.

Minke, B. and Kirschfeld, K. (1979). The contribution of a sensitizing pigment to the photosensitivity spectra of fly rhodopsin and metarhodopsin. *J Gen Physiol* **73**, 517-40.

Montell, C. (2012). *Drosophila* visual transduction. *Trends Neurosci* **35**, 356-63.

Montell, C. and Rubin, G. M. (1989). Molecular characterization of Drosophila *trp* locus, a putative integral membrane protein required for phototransduction. *Neuron* **2**, 1313-1323.

Nakatsu, F., Baskin, J. M., Chung, J., Tanner, L. B., Shui, G., Lee, S. Y., Pirruccello, M., Hao, M., Ingolia, N. T., Wenk, M. R. et al. (2012). PtdIns4P synthesis by PI4KIIIalpha at the plasma membrane and its impact on plasma membrane identity. *J Cell Biol* **199**, 1003-16.

Park, Y., Seo, J. B., Fraind, A., Perez-Lara, A., Yavuz, H., Han, K., Jung, S. R., Kattan, I., Walla, P. J., Choi, M. et al. (2015). Synaptotagmin-1 binds to PIP-containing membrane but not to SNAREs at physiological ionic strength. *Nat Struct Mol Biol* **22**, 815-823.

Payrastre, B., Missy, K., Giuriato, S., Bodin, S., Plantavid, M. and Gratacap, M. (2001). Phosphoinositides : key players in cell signalling, in time and space. *Cell Signal* **13**, 377-87.

Phillips, A. M., Bull, A. and Kelly, L. E. (1992). Identification of a Drosophila gene encoding a calmodulin-binding protein with homology to the trp phototransduction gene. *Neuron* **8**, 631-42.

Polevoy, G., Wei, H. C., Wong, R., Szentpetery, Z., Kim, Y. J., Goldbach, P., Steinbach, S. K., Balla, T. and Brill, J. A. (2009). Dual roles for the *Drosophila* PI 4-kinase four wheel drive in localizing Rab11 during cytokinesis. *J Cell Biol* **187**, 847-58.

Quinn, K. V., Behe, P. and Tinker, A. (2008). Monitoring changes in membrane phosphatidylinositol 4,5-bisphosphate in living cells using a domain from the transcription factor tubby. *J Physiol* **586**, 2855-71.

Raghu, P., Coessens, E., Manifava, M., Georgiev, P., Pettitt, T., Wood, E., Garcia-Murillas, I., Okkenhaug, H., Trivedi, D., Zhang, Q. et al. (2009). Rhabdomere biogenesis in *Drosophila* photoreceptors is acutely sensitive to phosphatidic acid levels. *J Cell Biol* **185**, 129-45.

Raghu, P., Colley, N. J., Webel, R., James, T., Hasan, G., Danin, M., Selinger, Z. and Hardie, R. C. (2000). Normal phototransduction in *Drosophila* photoreceptors lacking an $InsP_3$ receptor gene. *Mol Cell Neurosci* **15**, 429-445.

Raghu, P., Yadav, S. and Mallampati, N. B. (2012). Lipid signaling in *Drosophila* photoreceptors. *Biochim Biophys Acta* **1821**, 1154-65.

Rohacs, T. (2009). Phosphoinositide regulation of non-canonical transient receptor potential channels. *Cell Calcium* **45**, 554-65.

Satoh, A. K., Xia, H., Yan, L., Liu, C. H., Hardie, R. C. and Ready, D. F. (2010). Arrestin translocation is stoichiometric to rhodopsin isomerization and accelerated by phototransduction in *Drosophila* photoreceptors. *Neuron* **67**, 997-1008.

Sengupta, S., Barber, T. R., Xia, H., Ready, D. F. and Hardie, R. C. (2013). Depletion of PtdIns(4,5)P_y underlies retinal degeneration in *Drosophila* trp mutants. *J Cell Sci* **126**, 1247-59.

Stauffer, T. P., Ahn, S. and Meyer, T. (1998). Receptor-induced transient reduction in plasma membrane PtdIns(4,5)P_2 concentration monitored in living cells. *Curr Biol* **8**, 343-346.

Stowers, R. S. and Schwarz, T. L. (1999). A genetic method for generating *Drosophila* eyes composed exclusively of mitotic clones of a single genotype. *Genetics* **152**, 1631-9.

Tan, J. and Brill, J. A. (2014). Cinderella story: PI4P goes from precursor to key signaling molecule. *Crit Rev Biochem Mol Biol* **49**, 33-58.

Tan, J., Oh, K., Burgess, J., Hipfner, D. R. and Brill, J. A. (2014). PI4KIIIalpha is required for cortical integrity and cell polarity during *Drosophila* oogenesis. *J Cell Sci* **127**, 954-66.

Varnai, P. and Balla, T. (1998). Visualization of phosphoinositides that bind pleckstrin homology domains: calcium- and agonist-induced dynamic changes and relationship to myo-[3H]inositol-labeled phosphoinositide pools. *J Cell Biol* **143**, 501-10.

Varnai, P., Gulyas, G., Toth, D. J., Sohn, M., Sengupta, N. and Balla, T. (2017). Quantifying lipid changes in various membrane compartments using lipid binding protein domains. *Cell Calcium* **64**, 72-82.

Wang, T. and Montell, C. (2006). A Phosphoinositide Synthase Required for a Sustained Light Response. *J Neurosci* **26**, 12816-12825.

Wu, L., Niemeyer, B., Colley, N., Socolich, M. and Zuker, C. S. (1995). Regulation of PLC-mediated signalling in vivo by CDP-diacylglycerol synthase. *Nature* **373**, 216-222.

Wu, X., Chi, R. J., Baskin, J. M., Lucast, L., Burd, C. G., De Camilli, P. and Reinisch, K. M. (2014). Structural insights into assembly and regulation of the plasma membrane phosphatidylinositol 4-kinase complex. *Dev Cell* **28**, 19-29.

Yau, K. W. and Hardie, R. C. (2009). Phototransduction motifs and variations. *Cell* **139**, 246-64.

Yin, H. L. and Janmey, P. A. (2003). Phosphoinositide regulation of the actin cytoskeleton. *Annu Rev Physiol* **65**, 761-89.

Zhang, C., Liu, M. S. and Xing, X. H. (2009). Temperature influence on fluorescence intensity and enzyme activity of the fusion protein of GFP and hyperthermophilic xylanase. *Appl Microbiol Biotechnol* **84**, 511-7.

Zhang, X., Wang, W. A., Jiang, L. X., Liu, H. Y., Zhang, B. Z., Lim, N., Li, Q. Y. and Huang, F. D. (2017). Downregulation of RBO-PI4KIIIalpha Facilitates Abeta42 Secretion and Ameliorates Neural Deficits in Abeta42-Expressing *Drosophila*. *J Neurosci* **37**, 4928-4941.

Figure legends

Fig. 1 PIP_2 and PI4P recovery time courses in control flies

(A) Tb^{R332H} YFP fluorescence in response to a 30 s blue excitation light measured from rhabdomere patterns in the deep pseudopupil of otherwise wild-type fly. In a fully dark-adapted fly (red trace) fluorescence decays over ~20s as PIP_2 is depleted and the Tb^{R332H} probe translocates out of the rhabdomere. After M to R reconversion by red (R) light and variable periods in the dark: (Δt = 10 s - 200 s), the blue excitation was repeated and the return of the probe to the rhabdomeres (reflecting PIP_2 resynthesis) monitored from the instantaneous fluorescence (arrows). (B) Similar protocol from a fly expressing one copy of *GMR-Gal4* and UAS-*wRNAi* (*GMRw* control for RNAi experiments). **(**C,D) Similar traces from flies expressing the PI4P-specific P4M-GFP probe on wild-type (C) and *GMRw* (D) backgrounds**. (**E,F) Normalised time course of recovery from traces as in (A-D) after varying times in the dark: (E) PIP_2 monitored with Tb^{R332H}; mean ± s.e.m. n = 17 (wt), 27 (*GMRw*), (F) PI4P monitored with P4M (n = 9) . (G,H) Time for 50% recovery (t ½) for Tb^{R332H} (G) and P4M (H) probes (from timecourse data as in E and F). For both PIP_2 (Tb^{R332H}) and PI4P (P4M). There were distinct effects on kinetics of depletion and recovery attributable to GMR-Gal4 expression, emphasising the need for *GMR-Gal4* controls for UAS-RNAi experiments. (I) The canonical phosphoinositide cycle with identified and candidate genes indicated.

Fig. 2 PIP_2 and PI4P recovery time courses in RNAi flies

Time courses of Tb^{R332H} (A) and P4M (C) recovery in flies expressing RNAi constructs for various candidate genes under control of *GMR-Gal4* (mean ± s.e.m.). (B & D) time to 50% recovery (t½) for resynthesis of both PI4P (P4M) and PIP_2 (Tb^{R332H}) were substantially and significantly slowed in flies expressing UAS-RNAi constructs directed against *PI4KIIIα, rbo, YPP1, dPIP5K, dPIS* and *cds* (p < 0.0001, 1-way ANOVA, Dunnett's multiple comparison test). P4M data for cds^{KK} not shown as there was no detectable recovery. RNAi directed at other candidate PI4kinases (*fwd* and *PI4KIIα*), or either fly homologue of TMEM150A (CG4025 and CG7790 data pooled) had little or no effect. Flies were progeny of crosses between Tb^{R332H};*GMRw* or P4M;*GMRw* and the respective VDRC RNAi lines or the progenitor control (KK).

Fig. 3 Electroretinogram (ERG) recordings

(A) ERG responses to 1s flashes of increasing intensity in *GMRw* x *UAS-PI4KIIIα*-RNAi flies (n=5) and *GMRw* controls (n = 8). (B) Resulting response intensity functions (mean ± s.e.m.). Maximum intensity (10^0) was equivalent to ~ 10^7 effectively absorbed photons/sec. (C) ERG from *PI4KIIIα*-RNAi fly exposed to PIP_2 depleting stimulus (30 s saturating blue excitation followed by 5 s red light

to photoreisomerise M to R). Repeated brief (250 ms) dim red test flashes monitored loss and recovery of sensitivity. Inset shows similar protocol in a *GMRw/+* control fly. (D) Normalised time course of recovery following PIP_2 depleting stimuli from *PI4KIIIα*-RNAi flies and also from *YPP1*-RNAi, cds^{KK}-RNAi, *rbo*-RNAi, rbo^{ts} at 37°C (n = 4-10 flies as indicated) as well as rbo^{ts} at 22° C, *GMRw* and RNAi parent controls (n = 6 each).

Fig. 4 PIP_2 and PI4P resynthesis in rbo^{ts} mutants is blocked at 37° C .

(A-C) representative fluorescence traces from wild-type (A) and rbo^{ts} mutants expressing Tb^{R332H} to monitor PIP_2 (B) and P4M to monitor PI4P (C). Red traces are from initial dark-adapted state and the remaining traces after different times in the dark following depletion (5-200 s as indicated). Top series of traces at room temperature (22° C), bottom traces after warming to 37° C for 3 minutes. (A) In wt both depletion and recovery were markedly accelerated at 37° C; (B): in rbo^{ts}, Tb^{R332H} depletion was similarly accelerated at 37° C (red traces), but the apparent partial recovery now showed an increase during blue excitation rather than decay. (C) Most P4M fluorescence was already lost during the 3 minute warming period in the dark, and thereafter no recovery could be detected. The lower traces (A-C measured at 37°C) have been corrected (i.e. increased) for the 20% reduction in GFP fluorescence at 37°C. (D,E) Averaged recovery time courses for Tb^{R332H} and P4M from data as in **(**A-C) normalised to peak fluorescence. Plots show the mean ± s.e.m. from n = 8-14 flies per plot. (F) Time to 50% recovery (*t½*) for Tb^{R332H} (PIP_2) and P4M (PI4P) from plots for each fly. Note acceleration of recovery of both in wild-type at 37°C and slower recovery for P4M in rbo^{ts} compared to wild-type at the permissive temperature (22°C). *t½* data for rbo^{ts} at 37°C not shown because no flies recovered sufficient fluorescence.

Fig. 5 *In vivo* PIP_2 dynamics are barely affected in *dPIP5K* mutant or overexpressing eyes

(A) Normalised PIP_2 resynthesis time courses measured with Tb^{R332H} probe from mosaic $dPIP5K^{18}$ mutant eyes (mean ± s.e.m. n = 23 flies), compared to heterozygote siblings (n=23) and wild-type controls recorded on same days (n =13). (B) Recovery time course from flies overexpressing *dPIP5K* (oe) (driven by Rh1Gal4 n = 10) compared to sibling controls (non-Rh1Gal4 F1 from same cross) or Rh1Gal4;Tb^{R332H} parent controls pooled (n = 7). (C) Summary of time to 50% recovery (*t½*) of PIP_2 (i.e. Tb^{R332H}-YFP fluorescence) in $dPIP5K^{18}$ mosaics and overexpressing flies. On average, PIP_2 resynthesis time courses in $dPIP5K^{18}$ mosaic eyes were slightly slower than in controls, but data showed considerable overlap, reaching statistical significance only with respect to wild-type, but not sibling heterozygote controls.

Fig. 6 ERG recordings from *dPIP5K^{18}* mosaics

(A,B) Representative electroretinogram (ERG) responses to 1s flashes of increasing intensity from *dPIP5K^{18}* mosaic eyes and *dPIP5K^{18}*/+ sibling controls from the same cross. (C) *V*/log *I* function (ERG amplitudes at end of 1 s flash, mean ± s.e.m. n = 12); amplitudes were slightly reduced and sensitivity (intensity required to elicit 50% V_{max} response) ~3-fold reduced in mosaics, but the most conspicuous phenotype was the lack of "on" and "off" transients indicating that synaptic transmission was blocked. (D) ERG *V*/log *I* functions from *hdc* mutants, which also lack synaptic transmission (data replotted from Dau et al 2016), showed a similar reduction in amplitude and sensitivity compared to wild-type controls; however, this difference can be attributed to the lack of synaptic feedback to the photoreceptors. Maximum intensity (10^0) was equivalent to ~ 10^7 effective photons/sec.

Fig. 7 Whole-cell recordings from photoreceptors from *dPIP5K^{18}* mosaic eyes

Whole cell recordings from dissociated ommatidia from *dPIP5K^{18}* mosaic eyes (blue) and controls (*dPIP5K^{18}*/+, and wild-type recorded over the same time period pooled). (A) Responses to 1 ms flashes containing ~30 effective photons (means of responses from 10 flies) were virtually identical. (B) Peak amplitudes (p = 0.73 2-tailed unpaired t-test) and time-to-peak (p = 0.28) of responses were statistically indistinguishable. Red symbols are data from rare homozygote "escapers" .(C)Averaged quantum bumps (each is the average of 200-250 bumps from 4-5 cells, aligned by rising phase) in *dPIP5K^{18}* and control were again nearly identical. (D) Quantum efficiency and bump amplitudes (each point from a different cell) were statistically indistinguishable (p = 0.47. and 0.54 respectively). Red symbols: data from homozygote escapers (E) Responses to 1 sec flashes of light of increasing intensity: mean ± s.e.m. plotted in (F) for peak (above) and plateau (below, last 200 ms of response) were indistinguishable. n = 5 (*dPIP5K^{18}*) and 7 (control) cells.

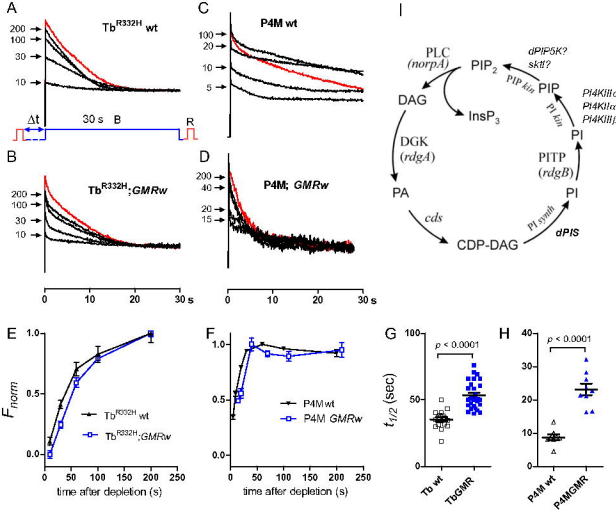
A
Tb^R332H wt
200
100
30
10
Δt
30 s
B
R
B
Tb^R332H;GMRw
200
100
30
10
C
P4M wt
100
20
10
5
D
P4M; GMRw
200
40
20
15
0
10
20
30 s
I
PLC
(norpA)
PIP2
dPIP5K?
skit?
PIP kin
PIP
DAG
InsP3
PI kin
PI4KIIIα?
PI4KIα?
PI4KIIIβ?
DGK
(rdgA)
PITP
(rdgB)
PI
PA
cds
PI synth
dPIS
CDP-DAG
E
F_norm
1.0
0.5
0.0
Tb^R332H wt
Tb^R332H;GMRw
0
50
100
150
200
250
time after depletion (s)
F
P4M wt
P4M GMRw
time after depletion (s)
G
t1/2 (sec)
100
50
p < 0.0001
Tb wt
TbGMR
H
40
30
20
10
p < 0.0001
P4M wt
P4MGMR

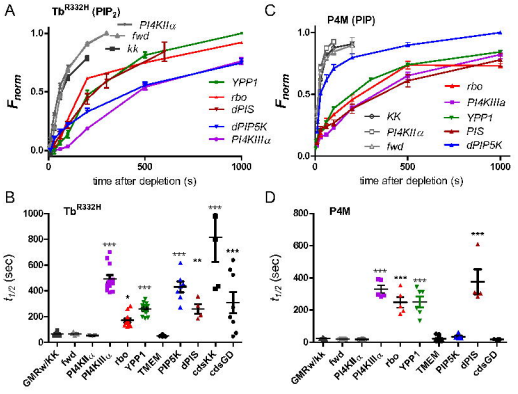
A
Tb^R332H (PIP2)
PI4KIIIα
fwd
kk
YPP1
rbo
dPIS
dPIP5K
PI4KIIIα
Fnorm
time after depletion (s)
B
Tb^R332H
t1/2 (sec)
GMRw/kk
fwd
PI4KIIIβ
PI4KIIIα
rbo
YPP1
TMEM
PIP5K
dPIS
cdsKK
cdsGD
C
P4M (PIP)
KK
PI4KIIIα
fwd
rbo
PI4KIIIa
YPP1
PIS
dPIP5K
Fnorm
time after depletion (s)
D
P4M
t1/2 (sec)
GMRw/kk
fwd
PI4KIIIβ
PI4KIIIα
rbo
YPP1
TMEM
PIP5K
dPIS
cdsGD

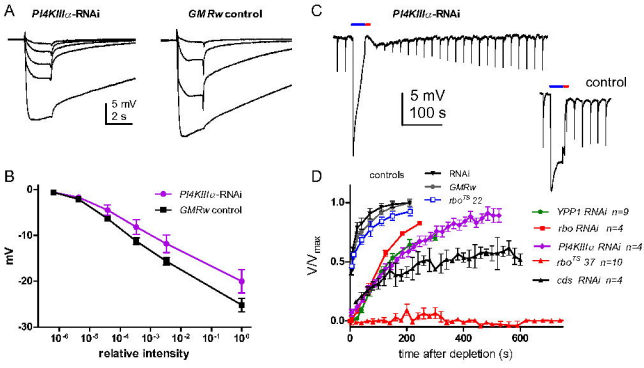
A
PI4KIIIα-RNAi
GMRw control
5 mV
2 s
B
PI4KIIIα-RNAi
GMRw control
mV
0
-10
-20
-30
10-6 10-5 10-4 10-3 10-2 10-1 100
relative intensity
C
PI4KIIIα-RNAi
5 mV
100 s
control
D
controls
RNAi
GMRw
rbo TS 22
V/Vmax
1.0
0.5
0.0
0 200 400 600
time after depletion (s)
YPP1 RNAi n=9
rbo RNAi n=4
PI4KIIIα RNAi n=4
rbo TS 37 n=10
cds RNAi n=4

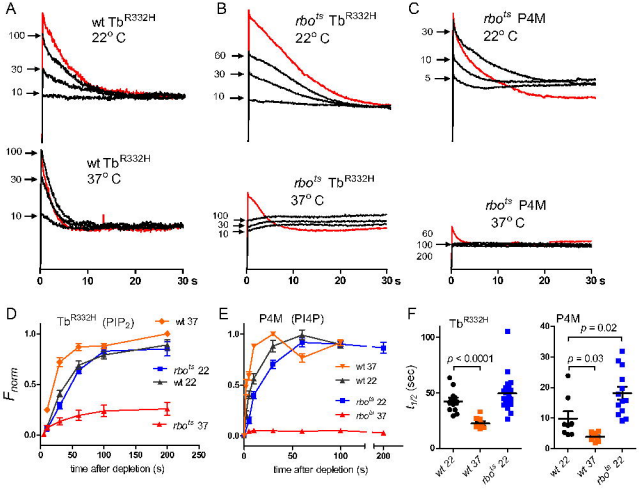
A
wt Tb^{R332H}
22° C
100
30
10
wt Tb^{R332H}
37° C
100
30
10
0
10
20
30 s
B
rbo^{ts} Tb^{R332H}
22° C
60
30
10
rbo^{ts} Tb^{R332H}
37° C
100
30
10
0
10
20
30 s
C
rbo^{ts} P4M
22° C
30
10
5
rbo^{ts} P4M
37° C
60
100
200
0
10
20
30 s
D
Tb^{R332H} (PIP$_2$)
wt 37
wt 22
rbo^{ts} 22
rbo^{ts} 37
F$_{norm}$
1.0
0.5
0.0
0
50
100
150
200
250
time after depletion (s)
E
P4M (PI4P)
wt 37
wt 22
rbo^{ts} 22
rbo^{ts} 37
1.0
0.5
0.0
0
50
100
200
time after depletion (s)
F
Tb^{R332H}
t$_{1/2}$ (sec)
100
50
0
p < 0.0001
wt 22
wt 37
rbo^{ts} 22
P4M
40
30
20
10
0
p = 0.03
p = 0.02
wt 22
wt 37
rbo^{ts} 22

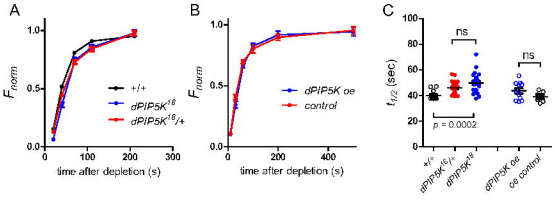
A
B
C
F_{norm}
1.0
0.5
0.0
0
100
200
300
400
time after depletion (s)
+/+
dPIP5K18
dPIP5K18/+
dPIP5K oe
control
$t_{1/2}$ (sec)
ns
p = 0.0002
+/+
dPIP5K18/+
dPIP5K18
dPIP5K oe
oe control

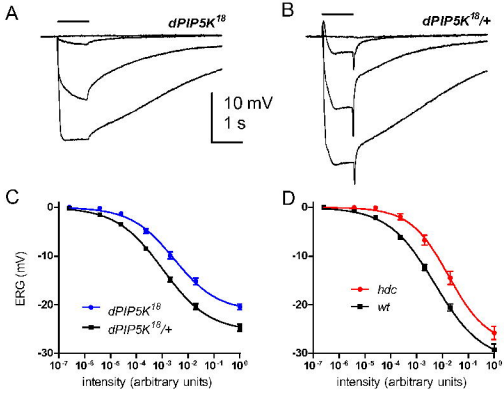
A
dPIP5K18
10 mV
1 s
B
dPIP5K18/+
C
ERG (mV)
0
-10
-20
-30
dPIP5K18
dPIP5K18/+
intensity (arbitrary units)
D
hdc
wt
intensity (arbitrary units)

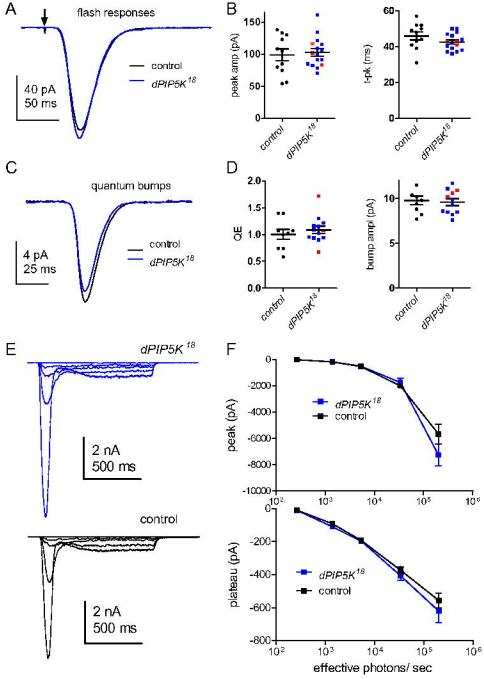
A
flash responses
control
dPIP5K18
40 pA
50 ms
B
peak amp (pA)
150
100
50
0
control
dPIP5K18
t-pk (ms)
60
40
20
0
control
dPIP5K18
C
quantum bumps
4 pA
25 ms
control
dPIP5K18
D
QE
2.0
1.5
1.0
0.5
0.0
control
dPIP5K18
bump amp (pA)
10
5
0
control
dPIP5K18
E
dPIP5K18
2 nA
500 ms
control
2 nA
500 ms
F
peak (pA)
0
-2000
-4000
-6000
-8000
-10000
dPIP5K18
control
10^2
10^3
10^4
10^5
10^6
plateau (pA)
0
-200
-400
-600
-800
dPIP5K18
control
effective photons/ sec